

WIND VELOCITY AND AEROSOL BACKSCATTER MEASURED BY CO₂ DOPPLER LIDAR

John R. Roadcap*, Robert A. Swirbalus, and Mitchell H. Laird
Phillips Laboratory, Geophysics Directorate Hanscom AFB, Massachusetts

Patrick J. McNicholl and David L. A. Rail
PhotoMetrics, Inc. Wobum, Massachusetts

1. INTRODUCTION

The real-time detailed vertical structure of wind velocity is of great interest to Air Force operations such as precision cargo drops and high altitude bomb delivery. Aerosols, clouds, and precipitation can also greatly affect the performance of optical sensors and weapons systems -- both passive and active -- from the visual through the long-wave infrared region.

To better understand the factors involved in real-time measurement of range-resolved wind velocity and aerosol backscatter under various atmospheric conditions, the Phillips Laboratory's Geophysics Directorate developed and fielded a ground-based eye-safe CO₂ Doppler lidar. The lidar has provided wind and aerosol backscatter profiles in support of several Department of Defense field programs including ballistic wind determination, high altitude cargo drops, post-detonation cloud tracking and diffusion, and high resolution ground-to-space imaging.

2. LIDAR DESCRIPTION

The Geophysics CO₂ Doppler lidar is a transportable pulsed heterodyne lidar system operating at a wavelength of approximately 10.6 μm . The laser lines are generated by Transverse Excited Atmospheric (TEA) CO₂ electric discharge lasers using an 80% mixture of buffer gases (He and N₂) with the CO₂. The laser output energy is about 60 mJ (60 x 10⁻³ Joules) with a pulse repetition frequency of 60 Hz. The laser scanning mirror possesses a hemispherical field-of-view. The range gates along the laser line-of-sight are approximately 150 meters. Characteristics of the CO₂ Doppler lidar are listed in Table I. In addition to measurement of the range-resolved

Phillips Laboratory CO ₂ Doppler Lidar	
Wavelength	10.6 μm
Pulse Energy	60-100 x 10 ³ Joules (mJ)
Pulse Rep. Frequency	10-100 S ⁻¹ (Hz)
Pulse Length	-1 x 10 ⁻⁴ s (μsec)
Range Gate Length	150 m
Laser	TEA Electric Discharge
Gas	CO ₂ with 80% mixture of N ₂ and He Buffer Gases
Telescope	30 cm Mersenne
Scanner	Hemispherical
Processor	Programmable DSP Array

Table 1. CO₂ Doppler lidar characteristics

radial wind component, the lidar also measures relative aerosol backscatter which can be used to determine the location of aerosols and clouds. As an example, a time-height cross-section of relative backscatter measured at

* Corresponding author address: Lt Col John R. RoadCap, USAF, PL/GPOL, 29 Randolph Road, Hanscom APB, Massachusetts 01731-3010 DSN 478-3016 fax: DSN 478-3661 e-mail: roadcap@plh.af.mil

Hanscom AFB by CO_2 Doppler lidar is shown in Figure 1. Regions of enhanced backscatter for this particular period were found near the atmospheric boundary layer below 1.5 km (AGL), within a relatively thick cirrus layer between 6 and 7 km, and in a thinner cirrus layer between 10 and 12 km.

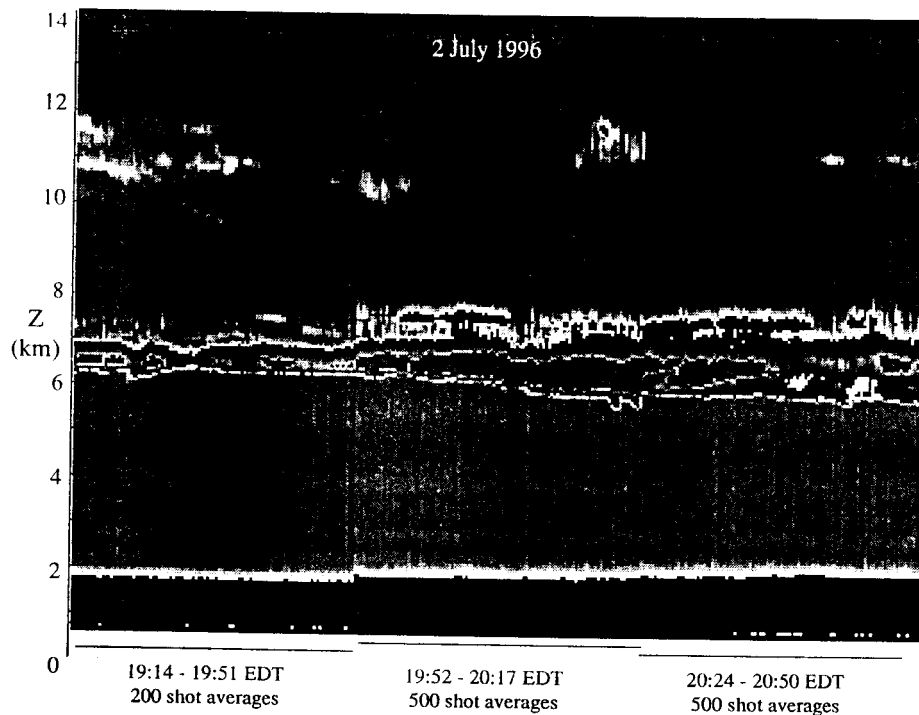


Figure 1. Time-height cross-section of relative backscatter measured by CO_2 heterodyne lidar at Hanscom AFB, Massachusetts on 2 July 1996

3. WIND VELOCITY DETERMINATION

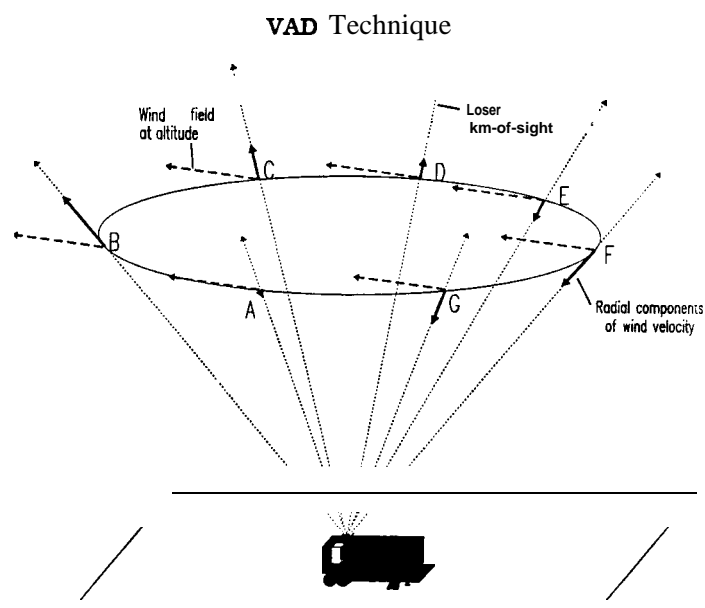


Figure 2. The Velocity-Azimuth Display (VAD) technique uses harmonic analysis of radial velocity as a function of azimuth angle to determine horizontal wind velocity

Because the Doppler **lidar** scanner possesses a hemispherical field-of-view and relies on ambient background aerosols for **backscatter**, the kinematic properties of the wind field in clear air (given sufficient **backscatter**) above the **lidar** can readily be determined under conditions where the wind field is homogeneous. The method used is the Velocity-Azimuth Display (**VAD**) technique (see Figure 2) which involves scanning the **lidar** about a vertical axis at a fixed elevation angle (Browning and Wexler, 1968). VAD curves of radial velocity as a function of azimuth angle are then constructed for each range gate. From the VAD curve coefficients, the horizontal wind vector and its kinematic properties can be computed at each range bin, and thus for a non-zero elevation angle scan, each altitude level.

Normally, at least 16 points or directions are used to construct each **VAD** scan consisting usually of 1000 laser shots per direction. The use of 16 points to construct the **VAD** curve is necessary to adequately represent the VAD curve such that measurement error is minimized consistent with the available **backscatter**. Figure 3 illustrates both the azimuthal and range distribution of radial velocity (part a.) and the construction of VAD curves for several range gates (part b) using 16 points. Alternating low (≤ 5 deg.) and high (~ 30 deg.) elevation angle scans are used to determine low level (near surface to 500 m) and higher level (200 m to 4 km) profiles of horizontal wind. A period of approximately five minutes is required to complete each scan.

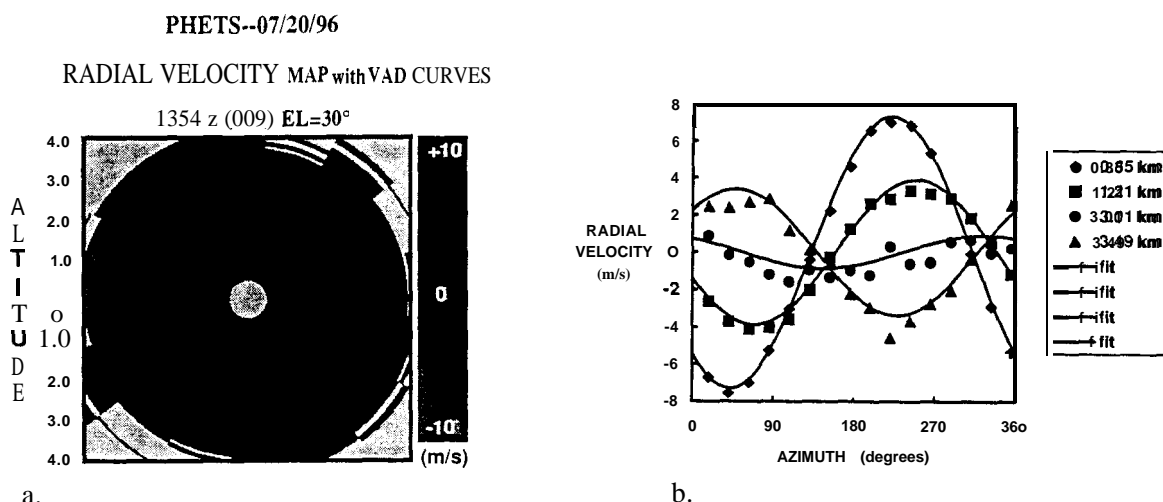


Figure 3. Construction of **VAD** curves for different range gates at 30 degree elevation angle. New Mexico, 20 July 1996

4. MEASUREMENT ACCURACY

The algorithm used to extract radial velocity **from** the Power Spectral Density (**PSD**) -- the square of the Fast Fourier Transform of the **lidar** pulse returns -- consists of two parts. The **first** is a search algorithm used to identify and locate the signal **spectral** feature in the PSD. Then, a **centroid** algorithm finds the central moment of the feature in some interval about this location. For example, the simplest and most often-used process seeks a maximum in the PSD and then calculates the centroid over a specified number of frequency intervals about this maximum.

In this two-step algorithm, there are two easily distinguishable Signal-to-Noise ratio (**SNR**) regimes. The **SNR** is defined here as the ratio of the sum of the signal over the **centroid** interval to the expected RMS variation of the corresponding sum of the noise power baseline. At **sufficiently** high **SNR**, the extraction accuracy is limited by the **centroid** analysis -- i.e., by the ability to determine the center **frequency** of a well-defined but noisy feature. As the **SNR** decreases, a point is reached where the search algorithm identification of the signal spectral feature becomes increasingly suspect. Below this **SNR**, the velocity measurement error can **drastically** increase. A typical velocity measurement error for sufficiently high **SNR** is ≤ 1 m/s.

Yuma, Arizona (Times MST)	Top (km-ACL)	Startire Range, N.M. (Times MDT)	Top (km-AGL)
6 March 1034	5.8	15 October 2315	2.5
7 March 1529	7.3	16 October 1950	4.5
8 March 1444	5.2	17 October 2138	2.5
8 March 1450	5.5	18 October 1928	2.5
9 March 1111	4.9	22 October 1420	1.5
9 March 1136	5.8	24 October 0120	2.5
9 March 1152	5.8	25 October 0053	3.0

Table 2. Apparent aerosol wind layer tops determined from CO₂ Doppler **lidar** during 1996

The **RMS** VAD deviation has two components: (1) a SNR-dependent part indicative of velocity extraction errors as discussed above, and (2) a SNR-independent part indicative of the atmospheric wind field deviations in the sampled volume from the homogeneous and horizontal model. With typical 16 azimuth point VAD scans and using prior knowledge gained from preceding VAD scans, we have found that reliable velocity extraction can be extended down to **SNRs** on the order of 4. Using this SNR threshold, in the absence of clouds, the upper height for wind **velocity** retrieval can vary widely depending on location and weather conditions. Table 2 illustrates examples of daily variation in upper height limit for wind retrieval by the CO₂ Doppler **lidar** associated with the rapid decrease in aerosol density above the surface.

5. MEASUREMENT RESULTS

5.1 *Synoptic Weather Overview*

Two recent series of observations have been selected to illustrate the CO₂ Doppler **lidar** measurement capability. The **first** set was taken in March 1996 near Yuma, Arizona where the dry stable troposphere was in general dominated by broad high pressure (see Figure 4). On the 6 of March, a strong, dry cold front ahead of a high pressure system centered over northern Nevada had just passed through the observation area. On 9 March, a west-

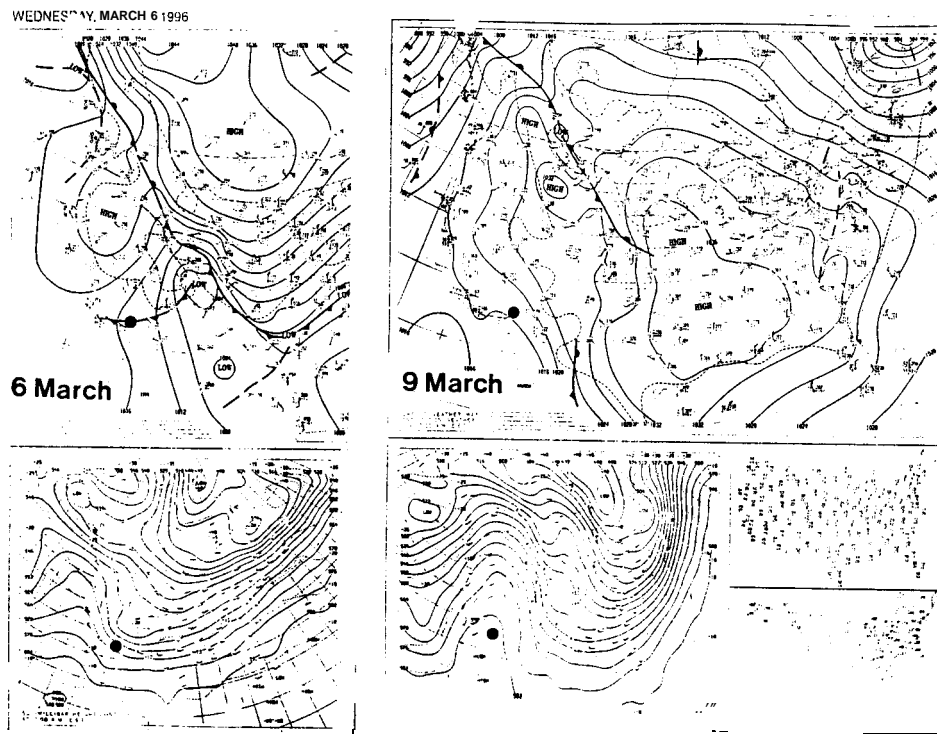


Figure 4. Surface and 500 mb. analyses for 12 GMT on 6 and 9 March 1996. “.” marks **lidar** observation site

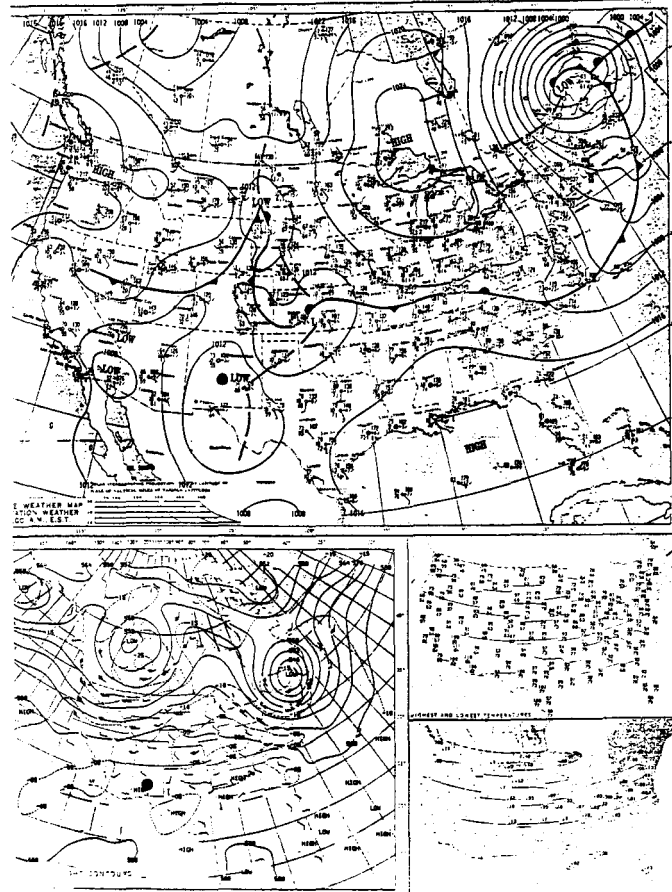


Figure 5. Surface and 500 mb. analysis for 12 GMT on 20 July 1996. “.” marks lidar observation site.

east sea level pressure gradient across southern Arizona was induced by an Arctic high centered over the Great Plains. Persistent thin cirrus associated with the subtropical jet stream was present during both days. The other set of observations was made during July 1996 in the **Jornado Del Muerto** region of New Mexico about 40 miles southeast of **Socorro**. The New Mexico observations occurred during the relatively moist summer season typically characterized by strong diurnal forcing with clear mornings and scattered afternoon thunderstorms. The sea level pressure gradient was very weak over this region (Figure 5).

5.2 Arizona March Observations

Two lidar measurement profiles of wind velocity and SNR from 6 and 9 March 1996 are shown in Figures 6 and 7 respectively. For 6 March, lidar observations show low level northwesterly flow between 5000 ft. and 10000 ft. AGL. A steady wind speed increase with height is also evident accompanied by strong backing above 10,000 ft. The SNR profile shows a sharp decrease with height such that the SNR threshold for useable radial velocity was being approached by 10,000 ft. Between 18,000 and 39,000 ft., the SNR values were too low ($\text{SNR} < 1.0$) to accurately compute radial velocity. Thus, the small SNR prevents the determination of horizontal wind velocity “using the VAD technique. Above 39,000 ft., sufficient backscatter from thin cirrus allowed determination of wind velocity to at least 43,000 ft. On 9 March, a low level easterly jet (which was also quite dry relative to the adjacent layers) was established below 5,000 ft. Above this level, wind speeds decreased up to 15,000 ft. where the flow became northwesterly. Most striking, however, are the much higher SNR values below 15,000 ft. when compared with the 6 March observations. Also, due to an invading thicker but lower cirrus layer, wind retrievals were possible up to 35,000 ft. except for a 5000 ft. layer of relatively low SNR just above 19000 ft. AGL.

Post Cold Front Passage -- Surface High over Nevada

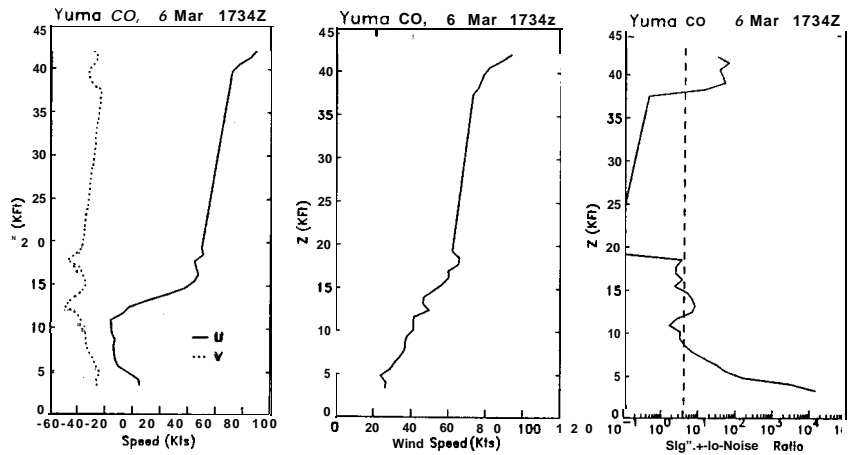


Figure 6. Wind velocity and Signal-to-Noise ratio vertical profiles for Yuma at 1734 GMT on 6 March.

Arctic High Over Plains -- Sharp Ridge Aloft

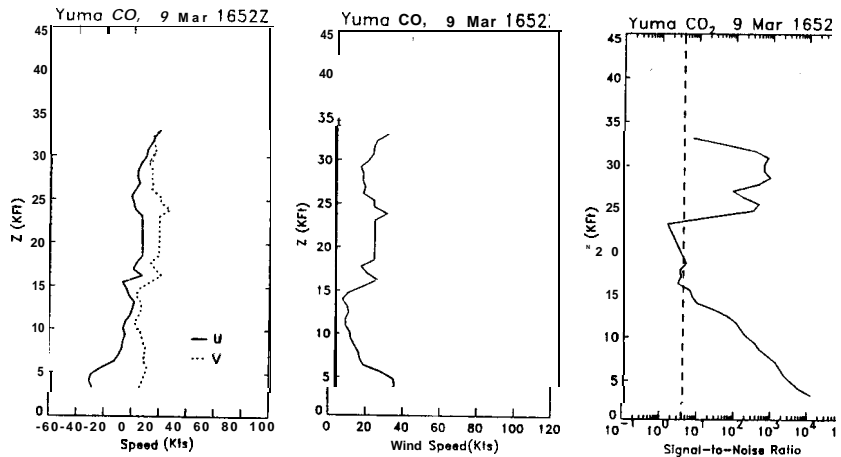


Figure 7. Wind velocity and Signal-to-Noise ratio vertical profiles for Yuma at 1652 GMT on 9 March.

5.2 New Mexico July Observations

A set of morning and afternoon VAD wind observations in and just above the boundary layer was made on 20 July 1996 in the Jomado Del **Muerto** region of south central New Mexico. These illustrate the Doppler **lidar's** ability to measure the rapidly changing wind profile as the boundary layer is modified both by insolation and afternoon thunderstorm activity. On the morning of 20 July, southern New Mexico was dominated by weak low pressure at the surface and weak high pressure aloft (see Figure 5). Skies remained clear overnight favoring **radiational** cooling of the boundary layer. The morning VAD wind profiles clearly show the evolution and decay of a low level jet (**LLJ**) centered **near** 800 m AGL (Figure 8). The LLJ is directed from SW-NE with a peak core speed of 16 knots. Above its core, the winds veer gradually to a NE direction by -3.5 km AGL. By 1630 GMT, the jet core rises to about 1 km and the peak speed is reduced to about 8 **knots**. A secondary wind maximum (**NW** direction) is located just below 2 km with a peak speed half that of the low level jet.

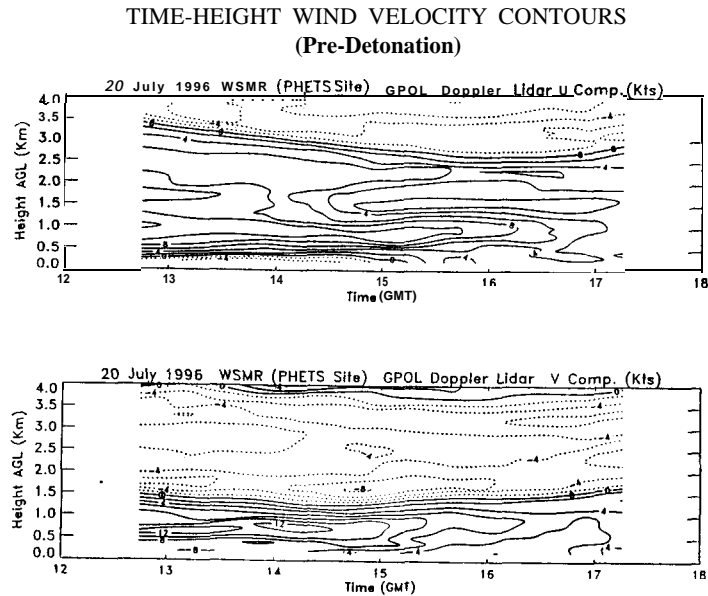


Figure 8. Time-height wind velocity structure measured by CO₂ Doppler lidar on morning of 20 July 1996.

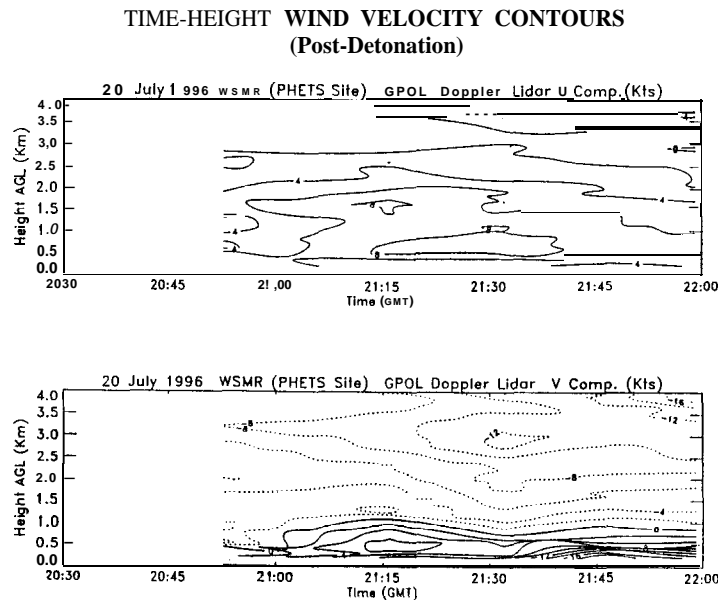


Figure 9. Time-height wind velocity structure measured by CO₂ Doppler lidar on afternoon of 20 July 1996.

The afternoon VAD wind profiles from 20 July are shown in Figure 9. They indicate a steady SW flow below 800 meters with wind speeds exceeding 18 knots near the surface by 2145 GMT. Above 800 m, winds of 8 knots **from** the NW were observed. The surge in the very low level surface flow just before 2145 GMT is caused by thunderstorm activity located south of the lidar site. Interestingly, a strong northerly surge of greater than 16 knots is observed near 4 km AGL prior to 2200 GMT. The sharp reversal of wind direction with height is evident also from a comparison of the 5 degree and 30 degree Plan Position Indicator (PPI) scans (not shown). Lidar observations terminated shortly after 2213 GMT.

VAD curves for 20 July (not shown) depict the transformation of the horizontal wind field from a smooth homogeneous structure prior to the decay of the low level jet to a broken inconsistent structure. This transformation including the decay of the low level jet is associated with the onset of both shallow convection within the boundary layer and deep convection. This is well illustrated in a comparison of Figure 10 and Figure 11. These figures display profiles of VAD Deviation (**RMS VAD Deviation**), discussed previously in Section 4, as

Morning Prior to Low Level Jet Decay

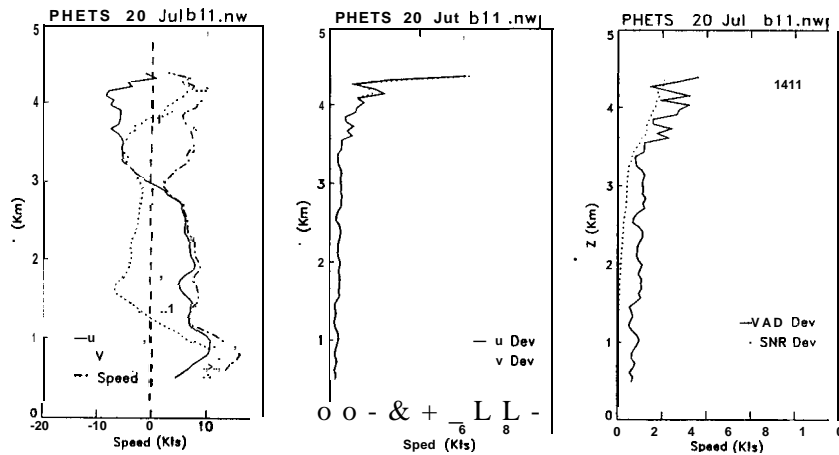


Figure 10. Vertical profiles of wind velocity and RMS VAD Deviation for 20 July at 1411 GMT measured by CO₂ Doppler lidar in south central New Mexico,

Afternoon Scattered Thunderstorms in Area

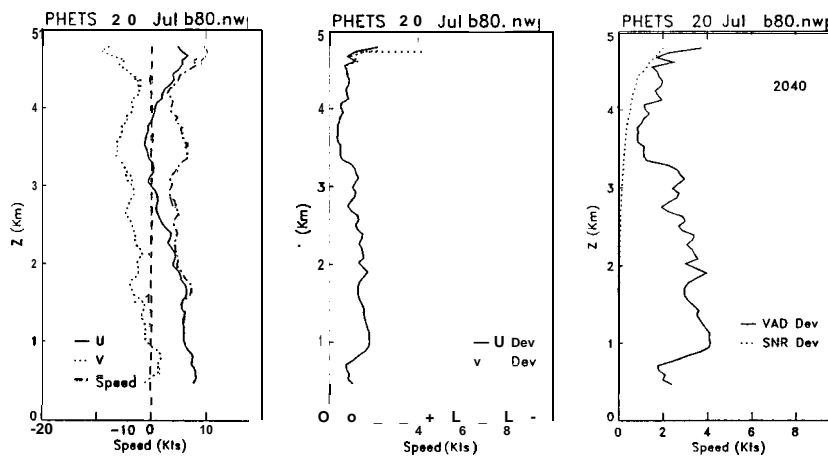


Figure 11. Vertical profiles of wind velocity and RMS VAD Deviation for 20 July at 2040 GMT measured by CO₂ Doppler lidar in south central New Mexico

well as profiles of the associated U and V wind components. In the morning prior to decay of the low level jet (-14 GMT), the VAD Deviation profiles are about 1 knot or less in magnitude below 3 km AGL (Figure 10). The increase above 3 km is primarily associated with an increase in the SNR Deviation associated with the rapid decrease in SNR and measurement accuracy of radial velocity. During the afternoon with scattered thunderstorms in the local area, the VAD Deviation increases by a factor of 3 or 4 below 3 km (Figure 11). This large increase is due almost solely to the SNR-independent component which is indicative of deviations in the observed wind field from the horizontally homogeneous assumptions of the VAD model.

6. SUMMARY AND CONCLUSIONS

CO₂ Doppler **lidar** measurements of range-resolved wind velocity and aerosol **backscatter** were shown for two measurement campaigns in the desert southwest U.S. -- one in the stable desert troposphere of late winter and the second during the moist, connectively unstable summer. Real-time wind velocity profiles in the lower troposphere were determined at about 10 to 15 minute intervals. Signal-to-Noise (SNR) ratios were also measured which estimate the aerosol **backscatter profiles**. Lidar measurements clearly revealed in both campaigns the distinct nature of the low level jet (LLJ) and, for the Arizona measurements, the presence of persistent cirrus in the upper troposphere. In Arizona, an aerosol "clean zone" of variable but considerable depth imposed significant limits on **lidar** wind retrieval in the mid-troposphere. Cirrus layers of considerable geometric thickness were observed during the Arizona tests within an altitude range of 25000 ft. -45000 ft. The Arizona LLJ core exhibited daily variation in speed, direction, altitude, and persistence related to changes in the large scale pressure gradient and low level stability. In the New Mexico observations, the CO₂ Doppler **lidar** revealed clearly the character of horizontal flow associated with diurnal changes in stability and convective activity.

The CO₂ Doppler **lidar** observations illustrate some of the capabilities and limitations of an eye-safe **ground-based IR heterodyne lidar** system. They also emphasize the importance of atmospheric factors in **lidar** wind sensing. The factors especially important are (1) the vertical distribution of aerosols **necessary** to provide sufficient backscatter and (2) horizontal flow variability, particularly in the boundary layer, and its relation to convective organization and terrain characteristics. Efforts are underway at the Geophysics Directorate to develop and employ **lidar** systems which measure wind velocity, absolute **backscatter**, and water vapor over greater vertical depths including the relatively aerosol-free regions of the middle troposphere.

7. REFERENCES

Browning, K.A. and R. Wexler, 1968: The determination of kinematic properties of a wind field using Doppler radar. *J. Appl. Met.*, 7,105-113.